JOURNAL OF MATERIALS SCIENCE 3 (1968) 47–60

Some Phase Relationships within the System $Na_2O/B_2O_3/Nb_2O_5$

D. BURNETT, D. CLINTON, R. P. MILLER
Division of Inorganic and Metallic Structure, National Physical Laboratory, Teddington, Middlesex, UK

Received 6 June 1967, and in revised form 24 August

Phase behaviour over regions of the ternary system $Na_2O/B_2O_3/Nb_2O_5$ has been explored.

Liquidus temperatures and the stability regions of primary phases have been determined over selected composition ranges by high temperature microscopy. Crystallisation processes in melts and corresponding glasses have been followed using both conventional methods of thermal analysis and newly developed micro techniques combined with hot stage microscopy.

An electron microscope has been employed to follow changes in the microstructure of quenched glasses after controlled heat treatments.

It has been shown that the system contains a liquid immiscibility gap, and some attention is given in the discussions to the influence that can be assigned to cations in determining the extent of such gaps and general structural relationships in borate/oxide systems.

1. Introduction

In this paper some general features of the behaviour of melts and glasses in the system $Na_2O/B_2O_3/Nb_2O_5$ are described. No previous work has been published on the chemistry of this ternary system, some aspects of which are considered to have wider implications for an understanding of fluxed growth mechanisms of producing single crystals from melts containing B_2O_3 as a constituent oxide. Compounds of the perovskite-type structure have received considerable attention over the last decade, because of their ferroelectric and optical properties and sodium niobate, $NaNbO_3$, is of particular interest since it is able to exhibit both ferroelectric and antiferroelectric properties [1, 2].

It was considered likely that a substantial area of the ternary diagram would have sodium niobate, $NaNbO_3$, as the primary phase. The delineation of this area, and its location with respect to the stability fields of other compounds in the system, was a primary objective of the work.

A secondary aim was the practical testing of new experimental methods, combining high temperature microscopy, thermal analysis and electron microscopy, which give direct information on crystallisation processes from the melts and the microstructural changes undergone by the glasses quenched from them.

To provide some background data to help in assessing the specific cation influence of niobium on the observed phase behaviour a brief comparative study was made on primary phase generation from diborate melts in which other oxides were substituted for Nb_2O_5. A summary of these results is tabulated before the more detailed work on the niobium system.

2. Experimental Procedure

2.1. Batch Preparation

All compounds used to prepare the melts were of either analytical grade, or of spectroscopically pure quality. Stock binary mixtures were prepared by mixing, grinding, sintering, or fusing the appropriate amounts of boric acid, sodium carbonate, or niobium pentoxide. The required quantities of the third component oxide was then added and the compositions homogenised by mechanical agitation in a "wig-L-bug" homogeniser.

Although mechanical agitation is sometimes

open to criticism as an effective means of mixing, confidence in this manner of preparing small batch quantities (1 g) for studies on the hot-stage microscope was established by the consistency of behaviour during multiple observations, and by checks with pre-fused and ground materials.

Fig. 1 shows the compositions investigated. All compositions are reported in mole %.

2.2. High Temperature Methods

High temperature microscopy was employed to supply the major part of the experimental data. This technique, and recent modifications which permit micro thermal analysis to be undertaken on the heated stage, have been described earlier [3, 4].

An induction furnace quenching assembly [5] was used for the preparation of bulk quantities (1 to 20 g) of borate glasses. For comparison the liquidus temperatures of selected compositions were determined by both techniques and the results shown to agree within $\pm 5°$ C.

In some cases the phenomenon of immiscibility in the melts was preserved during quenching to such an extent that fragments representative of the two stratified phases could be separated and independently examined.

On the macro scale, devitrification processes were followed by differential thermal analysis (DTA). Sample quantities were approximately 0.5 g of crushed powder, the heating rate being standardised at 10° C/min. Observations using DTA by hot stage microscopy [4] (μDTA) supplemented those made by orthodox DTA.

The course of the crystalline changes in the systems were established by X-ray powder photography.

2.3. Electron Microscopy Techniques

The electron microscope used was a JEM 7 instrument.

All specimens were examined by a two-stage replication technique. Bulk specimens were polished and etched with 2% HNO_3 solution. An impression was taken of the surface with an acetylcellulose film. On removal, the film was shadowed firstly with gold, and then with carbon, using conventional evaporation techniques. The carbon replica was then separated by dissolution of the acetylcellulose in methyl acetate.

The procedure was adapted to the examination of glass micro droplets after treatment in the high temperature microscope. The size of the beads, which were split off from the thermocouple micro-furnace, averaged 0.2 to 0.5 mm diameter.

3. Experimental Results

3.1. General Features of Some Oxide/Sodium Diborate Reactions

Preliminary explorations were made by high temperature microscopy on $Na_2B_4O_7$/metal oxide phase relationships. The study was in the nature of a very general survey of the broad features of the system's behaviour over the composition range 10 to 50 mole % metal oxide. The objective was to compare the crystallisation or glass-forming characteristics at equivalent concentrations in sodium diborate, of a variety of metal cations with inert gas configuration of differing field strengths.

Emphasis was placed on establishing the primary phase at equivalent concentrations (20 to 50% metal oxide) under comparable thermal treatments. No efforts were made to trace fully the equilibrium crystallisation paths, especially as many of the compositions formed stable glasses.

The findings are summarised in table I which also includes values for the field strength and common co-ordination numbers of the ions in oxide crystals.

TABLE I Primary phase in metal oxide/$Na_2B_4O_7$ systems (20 to 50% metal oxide).

Oxide	Field strength of cation†	Common co-ord. no. in oxides	Primary phase
Al_2O_3	0.86	4 or 6	*
Y_2O_3	0.56	6	Yttrium Borate
La_2O_3	0.46	6	Lanthanum Borate
TiO_2	0.93	6	Titanium Dioxide
ZrO_2	0.83	8	Zirconium Dioxide
ThO_2	0.72	8	Thorium Dioxide
V_2O_5	1.26	4	*
Nb_2O_5	1.14	6	Sodium Niobates
Ta_2O_5	1.14	6	Sodium Tantalates
MoO_3	1.48	6	Molybdenum Trioxide
WO_3	1.36	6	Tungsten Trioxide

*persistent glass
†field strength $= z/a^2$ where z is cation charge and a is cation-oxygen distance.

There are four main behaviour patterns:—

(*a*) *Formation of stable glass.* Nearly all the systems formed stable glasses at low metal oxide concentrations (~5 mole %), and in some (e.g. ZrO_2, HfO_2, MoO_3, and WO_3) the glass-

forming region was extended to higher concentrations. In the case of the Al_2O_3 and V_2O_5 systems, crystallisation from the melts or glasses could not be induced on the hot stage in spite of prolonged heat treatments at a variety of temperatures. The small sample size may be important here since Nador [6] has published a phase diagram of the system $V_2O_5/Na_2B_4O_7$ based on DTA investigations.

(*b*) *The metal oxide recrystallises.* With the thermal control which can be exercised with the hot stage microscope, well-formed single crystals can be grown from the melts.

(*c*) *The metal borate crystallises.* This occurred with yttrium and lanthanum oxides which are known to form borates in their respective B_2O_3 binary systems.

(*d*) With Nb_2O_5 and Ta_2O_5, compounds of the type $xNa_2O\ yM_2O_5$ crystallise from melts and glasses. This characteristic is apparently limited to these oxides, although according to the tentative equilibrium diagram $Na_2B_4O_7/V_2O_5$ advanced by Nador [6] vanadium may behave similarly.

It is of interest to note here that substituting Li^+ or Cs^+ for sodium in the above systems did not disturb the general pattern of phase behaviour outlined above.

3.2. The System $Na_2O/B_2O_3/Nb_2O_5$

3.2.1. The Limiting Binaries Na_2O/B_2O_3, Na_2O/Nb_2O_5, and Nb_2O_5/B_2O_3

Morey and Merwin [7] studied the system Na_2O/B_2O_3, and found over the composition range 0 to 50% Na_2O four compounds; $NaBO_2$, $Na_2B_4O_7$, NaB_3O_5, and $Na_2B_8O_{13}$. Supplementary devitrification and X-ray studies on glasses having compositions in this binary system relevant to the present work are described in section 3.3.1.

Shafer and Roy [8] investigated phase equilibria in the system Na_2O/Nb_2O_5. They characterised five compounds corresponding to formulae Na_3NbO_4, $NaNbO_3$, $Na_2Nb_8O_{21}$, $NaNb_7O_{18}$, and $Na_2Nb_{20}O_{51}$.

At the commencement of this present study there were no published data on the binary system Nb_2O_5/B_2O_3. This led to an exploration by hot stage microscopy which showed that the primary phase over a region of constant liquidus temperature (1345 $\pm$ 10° C) bounded approximately from 35 to 90% B_2O_3, was the high temperature polymorph of Nb_2O_5. Its generation was observed as a microcrystalline growth from the melts and it was identified by quenching and X-ray analysis.

The application of high temperature microscopy to studies on this system is limited by the problem of specimen volatility. However, evaporating specimens could be seen to have a constant liquidus temperature over the region stated, and it is considered that only at the extremities of this region is confidence in the accuracy of the liquidus profile measurements limited using this technique. The two-phase nature of the melts over this composition range was confirmed visually, being observable under the microscope as non-mixing areas of differing refractive index. These findings agree with the recently-published comprehensive phase diagram by Levin [9] who showed in addition that the compound $3Nb_2O_5.B_2O_3$ forms in sub-solidus regions $< 1155 \pm 15°$ C.

3.2.2. The Ternary Phase Diagram

Table II contains the phase data from the compositions studied arranged according to decreasing percentage of Na_2O. The locations of the compositions studied are shown in fig. 1, and the proposed phase diagram in fig. 2. In this figure the heavy lines, both solid and dashed, represent the phase boundaries and delineate the primary phase areas. The arrows indicate the direction of falling temperature. Isotherms are drawn generally at 100° C intervals.

Only two secondary binary systems were found: $NaNbO_3/NaBO_2$, and $NaBO_2/Na_3NbO_4$; the liquidus profile of the $NaNbO_3/NaBO_2$ sub-

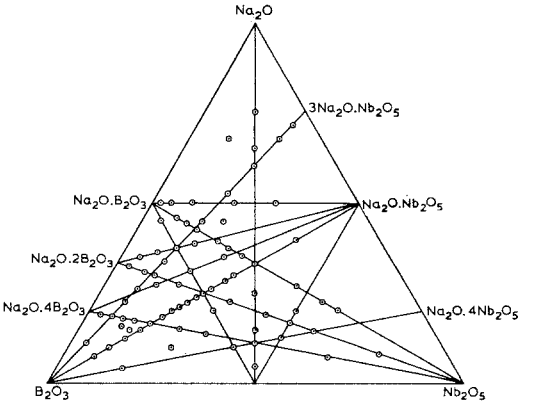

Figure 1 Compositions studied in the system $Na_2O/Nb_2O_5/B_2O_3$.

TABLE II Phase data from the compositions studied.

Mole % oxide			Liquidus	Primary phase	Secondary phase(s)
Na_2O	B_2O_3	Nb_2O_5	(° C)		
75	12.5	12.5	1040	Na_3NbO_4	—
71.5	5	23.5	990	Na_3NbO_4	—
67.5	22.5	10	818	(Na_3NbO_4 + $NaNbO_3$)	—
65	17.5	17.5	900	(Na_3NbO_4 + $NaNbO_3$)	$NaBO_2$
60	20	20	1150	$NaNbO_3$	Na_3NbO_4 + $NaBO_2$
52.5	30	17.5	1215	$NaNbO_3$	Na_3NbO_4 + $NaBO_2$
51	45	4	780	$NaNbO_3$ + (Na_3NbO_4 + $NaBO_2$)	—
50	47.5	2.5	977	$NaBO_2$	$NaNbO_3$
50	45	5	1050	$NaNbO_3$	$NaBO_2$
50	40	10	1116	$NaNbO_3$	$NaBO_2$
50	30	20	1260	$NaNbO_3$	$NaBO_2$
50	20	30	1380	$NaNbO_3$	$NaBO_2$
46	46	8	1040	$NaNbO_3$	$NaBO_2$
45	50	5	1000	$NaNbO_3$	$NaBO_2$
45	40	15	1215	$NaNbO_3$	—
45	35	20	1250	$NaNbO_3$	—
44.5	44.5	11	1190	$NaNbO_3$	—
42.33	42.33	14.33	1240	$NaNbO_3$	—
40	20	40	1350	$NaNbO_3$	
39.33	39.33	21.33	1250	$NaNbO_3$	—
38.75	44.5	15.75	1145	$NaNbO_3$	—
37.5	50	12.5	1175	$NaNbO_3$	—
37.5	37.5	25	1260	$NaNbO_3$	—
35.5	35.5	29	1320	$NaNbO_3$	—
35	60	5	1000	$NaNbO_3$	—
35	56	9	1015	$NaNbO_3$	—
34.75	55	11.25	1108	$NaNbO_3$	—
33.33	33.33	33.33	1340	$NaNbO_3$	$Na_2Nb_8O_{21}$
32	64.5	3.5	972	$NaNbO_3$	(unidentified phase)
31	50	19	1115	$NaNbO_3$	—
30.5	61.5	8	1039	$NaNbO_3$	—
30	40	30	1300	$NaNbO_3$	$Na_2Nb_8O_{21}$
29.66	50.33	11	1063	$NaNbO_3$	—
28	44	28	1130	$NaNbO_3$	$Na_2Nb_8O_{21}$
27.5	55	17.5	1073	$NaNbO_3$	$Na_2Nb_8O_{21}$
26.5	65	8.5	1043	$NaNbO_3$	—
26.5	26.5	47	1205	$NaNbO_3$	$Na_2Nb_8O_{21}$
26.25	47.5	26.25	1080	$NaNbO_3$	$Na_2Nb_8O_{21}$
25	50	25	1074	$NaNbO_3$	$Na_2Nb_8O_{21}$
25	37.5	37.5	1150	$NaNbO_3$	$Na_2Nb_8O_{21}$
24	52	24	1100	$NaNbO_3$	$Na_2Nb_8O_{21}$
23	70	7	935	$NaNbO_3$	—
22.5	55	22.5	1100	$NaNbO_3$	$Na_2Nb_8O_{21}$
22.5	22.5	55	1205	$Na_2Nb_8O_{21}$	$NaNbO_3$
22	45	33	1095	$NaNbO_3$	$Na_2Nb_8O_{21}$
21.33	57.33	21.33	1105	$Na_2Nb_8O_{21}$	$NaNbO_3$
20	60	20	1078	$Na_2Nb_8O_{21}$	$NaNbO_3$
20	50	30	1120	$Na_2Nb_8O_{21}$	$NaNbO_3$
20	30	50	1155	$Na_2Nb_8O_{21}$	$NaNbO_3$
20	20	60	1280	$Na_2Nb_8O_{21}$	$NaNbO_3$
19.33	77.33	3.33	845	($NaNbO_3$ + $Na_2Nb_8O_{21}$)	—
18.5	63	18.5	1085	$Na_2Nb_8O_{21}$	$NaNbO_3$
18.5	37.5	44	1070	$Na_2Nb_8O_{21}$	$NaNbO_3$
17.5	70	12.5	960	$Na_2Nb_8O_{21}$	$NaNbO_3$

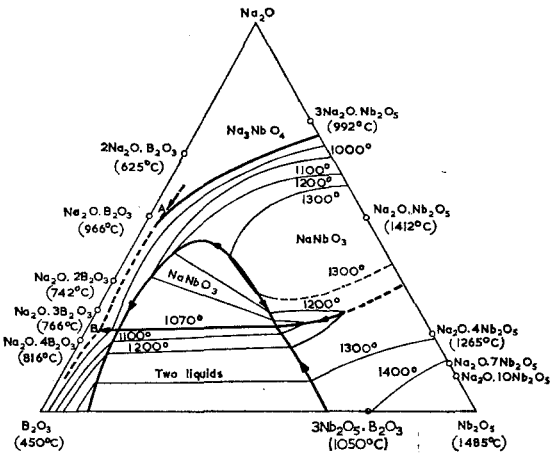

Figure 2 Ternary diagram of the system $Na_2O/Nb_2O_5/B_2O_3$.

system is shown separately in fig. 3a together with the liquidus profile of the pseudo-binary system $Nb_2O_5/Na_2B_4O_7$ (fig. 3b).

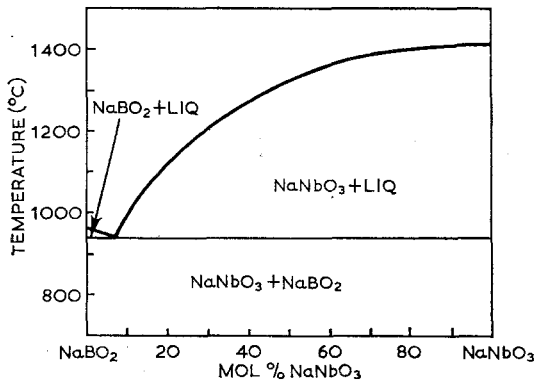

Figure 3a The section $NaNbO_3/NaBO_2$.

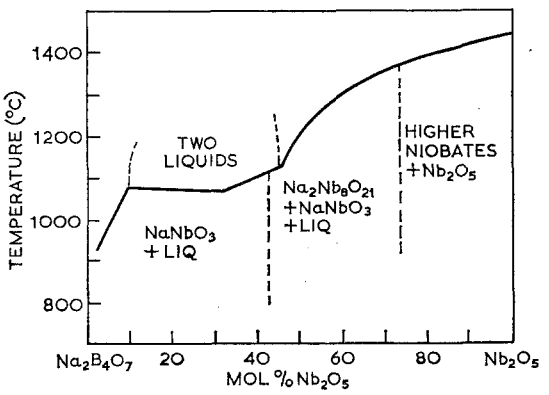

Figure 3b The section $Na_2B_4O_7/Nb_2O_5$.

The liquidus profile at low Nb_2O_5 contents (~3 mole %) is questionable because of persistent glass formation. Fig. 4 shows the region in which glass formation readily occurred on slow cooling (~10° C/min) and that portion of the diagram which on air quenching (500° C/sec) also produced an X-ray amorphous glass.

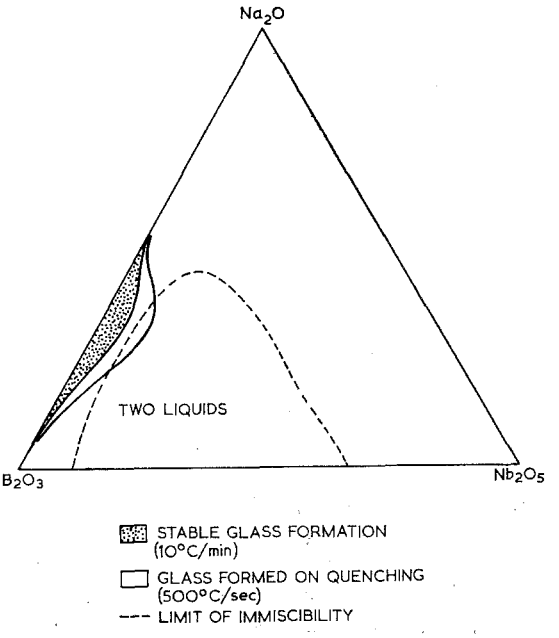

Figure 4 Glass forming tendency in the system Na_2O Nb_2O_5/B_2O_3.

For example, it was shown by thermal analysis in the high temperature microscope that glass formation along the join $Na_2B_4O_7/Nb_2O_5$ became increasingly difficult to achieve beyond 40 mole Nb_2O_5: 60 mole $Na_2B_4O_7$. Thus quenching rates of 250° C/sec, 500° C/sec, and 800° C/sec were required to produce clear glasses at the respective mole ratios Nb_2O_5: $Na_2B_4O_7$ of 20:80; 30:70; and 40:60. At slower cooling rates microcrystalline dispersions of sodium niobate ($NaNbO_3$) formed.

The areas in which sodium diborate and other sodium borate phases have stability, could not be well defined because of sluggish crystallisation characteristics. It has been convincingly demonstrated that only when finely crushed glasses are heated in bulk does crystallisation of sodium borate compounds occur. Evidence of this surface dependent nucleation is presented in detail when describing the DTA studies on quenched glasses. Since a devitrification tempera-

ture in a glass need bear no relation to a true equilibrium reaction temperature, it is only possible, on DTA evidence, to indicate that sodium borates are compatible with sodium niobates in the sub-solidus regions.

In the diborate-rich region ($\sim 2\%Nb_2O_5$) of the $Na_2O.2B_2O_3/Nb_2O_5$ binary an unidentified crystalline material, growing as highly birefringent dendritic clusters, emerged as the primary phase. The X-ray powder pattern did not conform to any known niobate or borate. This is one feature of the system which is still unresolved, another being the detailed phase relationships at the niobium-rich end of the diagram. The X-ray powder photographs indicated that the phases in this region include $Na_2O.4Nb_2O_5$, $Na_2O.7Nb_2O_5$, $Na_2O.10Nb_2O_5$, and Nb_2O_5, but their primary phase fields were not delineated.

Few data could be obtained in the regions rich in Na_2O due to volatilisation, and rapid hydration of the samples after quenching. However, the location of the ternary eutectic point (point A in fig. 2) between Na_3NbO_4, $NaBO_3$, and $NaNbO_3$ was established at 4.0% Nb_2O_5 : 45% B_2O_3 : 51% Na_2O, at 780 $\pm$ 10° C.

Primary crystallisation from melts in the sodium niobate field occurred readily except in the case of a few compositions located near the sodium tetraborate boundary. Well formed cubic crystals of $NaNbO_3$ could be grown on the hot-stage microscope, as seen in fig. 5.

The two polymorphic inversions of $NaNbO_3$ cubic → tetragonal occurring at 640° C, and the tetragonal → orthorhombic occurring at 368° C, could be observed under the hot-stage microscope by birefringence colour changes, the lower temperature transformation being particularly well marked.

3.3. Devitrification of Glasses in the Sodium Diborate/Niobium Pentoxide Subsystem

Studies were undertaken on both microscopic and macroscopic quantities of quenched glasses, to follow phase separation and crystal growth processes as a function of heat treatment. Attention was confined to the subsystem $Na_2O.2B_2O_3/Nb_2O_5$, and in particular to that portion of the diagram in which $NaNbO_3$ was the primary phase.

Glasses prepared on the 20 g scale in platinum crucibles frequently stratified into two layers. The batches were therefore homogenised by crushing, grinding and mixing before thermal analytical studies. The immiscible nature of the systems is discussed more fully in section 3.3.2.

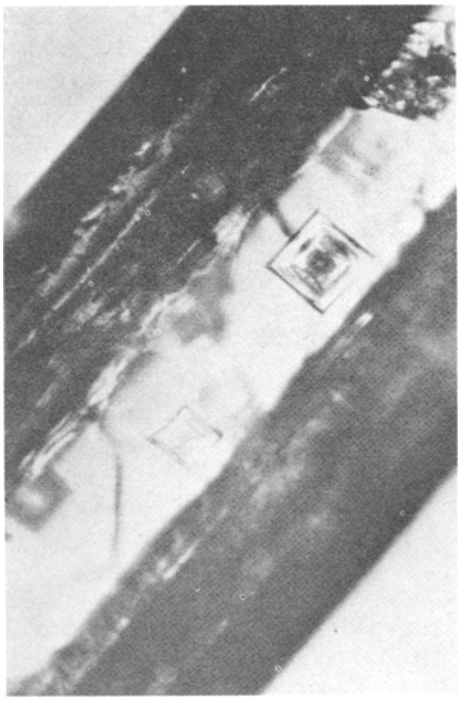

Figure 5 Cubic crystals of $NaNbO_3$ grown on the hot-stage microscope (×125).

3.3.1. Differential Thermal Analysis and X-ray Analysis

The differential thermograms of 0.5 g quantities of powdered quenched glasses of respective mole compositions 20% Nb_2O_5 : 80% $Na_2B_4O_7$, 30% Nb_2O_5 : 70% $Na_2B_4O_7$, 40% Nb_2O_5 : 60% $Na_2B_4O_7$ are shown in fig. 6.

The thermograms indicate a complex series of phase changes. Common to all is a strong exothermic reaction commencing at 560 to 580° C. This increases in magnitude as the Nb_2O_5 content of the glasses is increased. This heat effect can be confidently assigned to the crystallisation of $NaNbO_3$. In the glasses of higher niobium content (30 to 40% Nb_2O_5) a smaller sharp exotherm at 470° C preceded the main exotherm occurring at 560 to 580° C.

The exotherm at 650° C can be assigned to the devitrification of sodium diborate ($Na_2B_4O_7$). Thus X-ray analysis of the 30% Nb_2O_5 composition after this third heat effect showed that all the lines on the powder photograph, apart from some weak unidentified reflections were attribu-

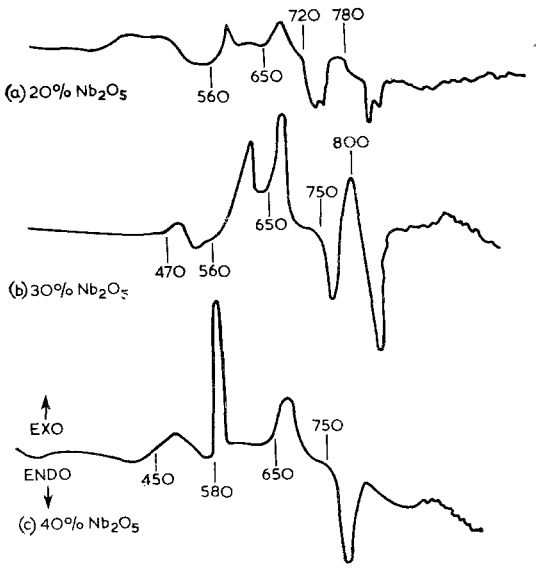

Figure 6 Macro differential thermograms of Nb_2O_5/$Na_2B_4O_7$ powdered quenched glasses.

table to $NaNbO_3$ and sodium diborate. The sodium diborate growth was found to be dependent on a large surface area as shown by DTA on a block of glass (30% Nb_2O_5). No exotherm occurred at 650° C and X-ray analysis confirmed the absence of sodium diborate.

The endotherm commencing between 720 to 750° C (fig. 6), when powdered samples were used, is assigned to the fusion of sodium diborate. As expected, on this assignment the endotherm is absent on the thermograms of bulk glasses in the $Nb_2O_5/Na_2B_4O_7$ system, where $Na_2B_4O_7$ fails to crystallise. Further confirmation was afforded by DTA on a pure glass of composition $Na_2O.2B_2O_3$. The thermogram is shown in fig. 7a, which shows that sodium diborate devitrifies at 520° C (confirmed by X-ray analysis) and redissolves at 740° C.

The endotherm at 800° C, most marked at the 30% Nb_2O_5 composition and absent in the 40% Nb_2O_5 composition, is of uncertain origin. This temperature is approximately 200° C below the liquidus (cf fig. 3b), and it was in fact confirmed by observations under the hot stage microscope that no dissolution of the sodium niobate microcrystals was occurring at this temperature. The fusion of other borate phases was considered as a possible origin of the 800° C endotherm. The two most likely phases would be either $Na_2O.3BO_3$, or $Na_2O.4B_2O_3$. Reference

TABLE III X-ray powder data on the crystallised glasses $Na_2O.4B_2O_3$ and $Na_2O.3B_2O_3$.

$Na_2O.4B_2O_3$		$Na_2O.3B_2O_3$	
I*	d(Å)	I*	d(Å)
vvw	8.46	mw	7.72
vw	4.44	w	7.13
vvw	3.99	w	6.63
w	3.34	w	6.12
mw	3.22	m	4.86
vvw	3.12	m	4.75
s	3.00	mw	4.37
s	2.91	s	3.71
vw	2.708	m	3.02
mw	2.544	m	2.93
m	2.513	ms	2.84
vw	2.017	m	2.63
w	1.679	mw	2.39
m	1.621	w	2.28
w	1.513	w	2.18
mw	1.418	vw	2.13
vvw	1.340	m	2.03
vvw	1.274	w	1.96
		ms	1.88
		w	1.87
		w	1.77

*v = very; m = medium; s = strong; w = weak.

thermograms of two pure glasses of these compositions were recorded (fig. 7b, c) and the X-ray powder data tabulated (table III). Although both glasses show endotherms close to 800° C neither of these crystalline phases were detected in the devitrified niobium-containing systems, ruling out the possibility of their being involved in the change. This leaves in some question the origin of the 800° C endotherm in the $Nb_2O_5/Na_2B_4O_7$ glass.

Studies using μDTA revealed features of phase change which were not possible to define by bulk thermal analysis. The heating rates which can be commanded are higher, thereby increasing the definition of heat effects, although this may occur at the expense of resolution, and reaction temperatures are usually displaced to higher values.

Thermograms of the compositions 20% Nb_2O_5 : 80% $Na_2B_4O_7$, 30% Nb_2O_5 : 70% $Na_2B_4O_7$, and 40% Nb_2O_5 : 60% $Na_2B_4O_7$ at a heating rate of 250° C/min are shown in fig. 8. The thermogram of the 20% Nb_2O_5 composition shows that no detectable heat effect is associated with the relatively sluggish growth of $NaNbO_3$ at 640° C. Visual observation showed no change in the specimen until this temperature.

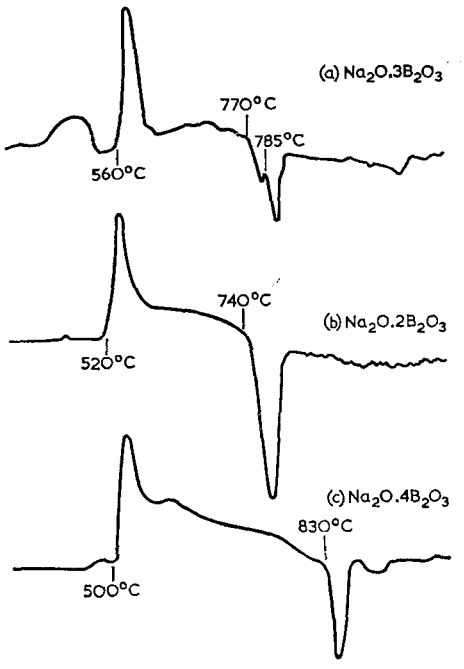

Figure 7 Reference thermograms of binary Na_2O/B_2O_3 powdered quenched glasses.

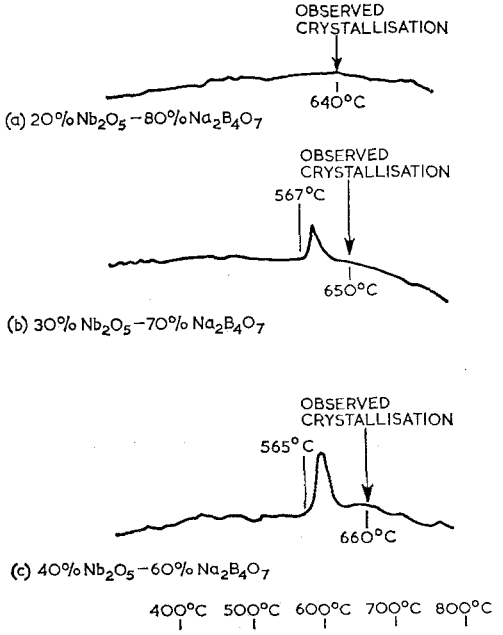

Figure 8 Micro thermograms of $Nb_2O_5/Na_2B_4O_7$ quenched glasses.

Preceding the precipitation of $NaNbO_3$ in glasses of the 30% Nb_2O_5 composition, a well defined exotherm occurs at 567° C. No visible change other than an apparent increase in specimen volume was associated with this precrystallisation phenomena. X-ray analysis of specimens, quenched immediately after this effect, confirmed that the system had remained X-ray amorphous. Electron microscopy, however (see section 3.3.2), revealed suggestive evidence of a microstructural change.

Microcrystalline growth of $NaNbO_3$ followed these changes. Apart from a change of slope in the ΔT base line no heat effect accompanied this crystallisation. No borate phase crystallised on the hot stage, and there were no heat effects corresponding to those found during macro DTA. The same pattern of behaviour was followed by the 40% Nb_2O_5 glass, the precrystallisation exotherm being larger.

It is reasonable to suppose that the precrystallisation exotherm effect at 470° C, found by macro DTA on the 30 and 40% Nb_2O_5 glasses, corresponds to the precrystallisation exotherm occurring on μDTA at 565° C, the displacement to higher temperatures arising from the greatly increased heating rate. This was confirmed by slower heating schedules which reduced this reaction temperature. The lack of any noticeable heat effect associated with $NaNbO_3$ crystallisation on the hot stage, and the complete absence of any borate crystallisation, must be attributed to the differences in specfiic surface between the microdroplets and the crushed powder used in the macro instrument. The size of the beads usually lies between 0.2 and 0.5 mm diameter, whereas the powdered glass (−300 BS mesh) was 50 μm. The crushed glass thus has a specific surface of one or two orders of magnitude greater than the beads. This promotes more ready crystallisation than can sometimes be induced on the hot stage.

3.3.2. Electron Microscope Studies

Electron micrographs of quenched specimens whose compositions lie outside the immiscibility gap were generally featureless. The two-phase nature of a bulk sample of a quenched glass of composition 40% Nb_2O_5 : 60% $Na_2B_4O_7$ is shown in fig. 9. In this case the niobium-rich phase is characterised by crystallites (~1000 Å) of sodium niobate, which are generated at all quenching rates < 800° C/sec. The crystallites develop on heat treatment at 600° C into the

typical cubic habit of this compound (fig. 11).

The glass-in-glass separation, which precedes the microcrystalline generation of sodium niobate, was illustrated during heat treatment of a quenched bulk glass of composition 30% Nb_2O_5 : 70% $Na_2B_4O_7$. The immiscible nature of the quenched product is shown in fig. 10. On heat treatment at 600° C the globules transform into cubic crystals of sodium niobate ($NaNbO_3$) (fig. 11).

The borate-rich glass remained homogeneous during heat treatment at 600° C (fig. 12a). At 675° C some structure becomes evident in the glass (fig. 12b) prior to crystallisation of sodium diborate, the crystals of which emerge with irregular habit (fig. 12c).

In an attempt to understand the significance of the precrystallisation exotherm observed during the thermal analysis studies on the glasses (section 3.3.1), quenched beads (40% Nb_2O_5 : 60% $Na_2B_4O_7$) from the the μDTA were examined under the electron microscope before and after the exotherm at 567° C (refer to fig. 8c). The generally immiscible character of the microstructure before this exotherm (cf. fig. 10) became transformed into an extensive featureless fine structure at 600° C (fig. 13). Recalling that the specimen at this stage is X-ray amorphous, it is presumed that the appearance of this microstructure, and the accompanying heat effects, are phenomena associated with the nucleation of sodium niobate, which subsequently precipitates at 640° C in the form of a featureless cloud of microcrystals. This conclusion, however, is speculative.

3.4. Growth Characteristics of Sodium Niobate from Sodium Diborate

By use of the hot stage microscope it was possible to obtain quantitative growth rate data for the

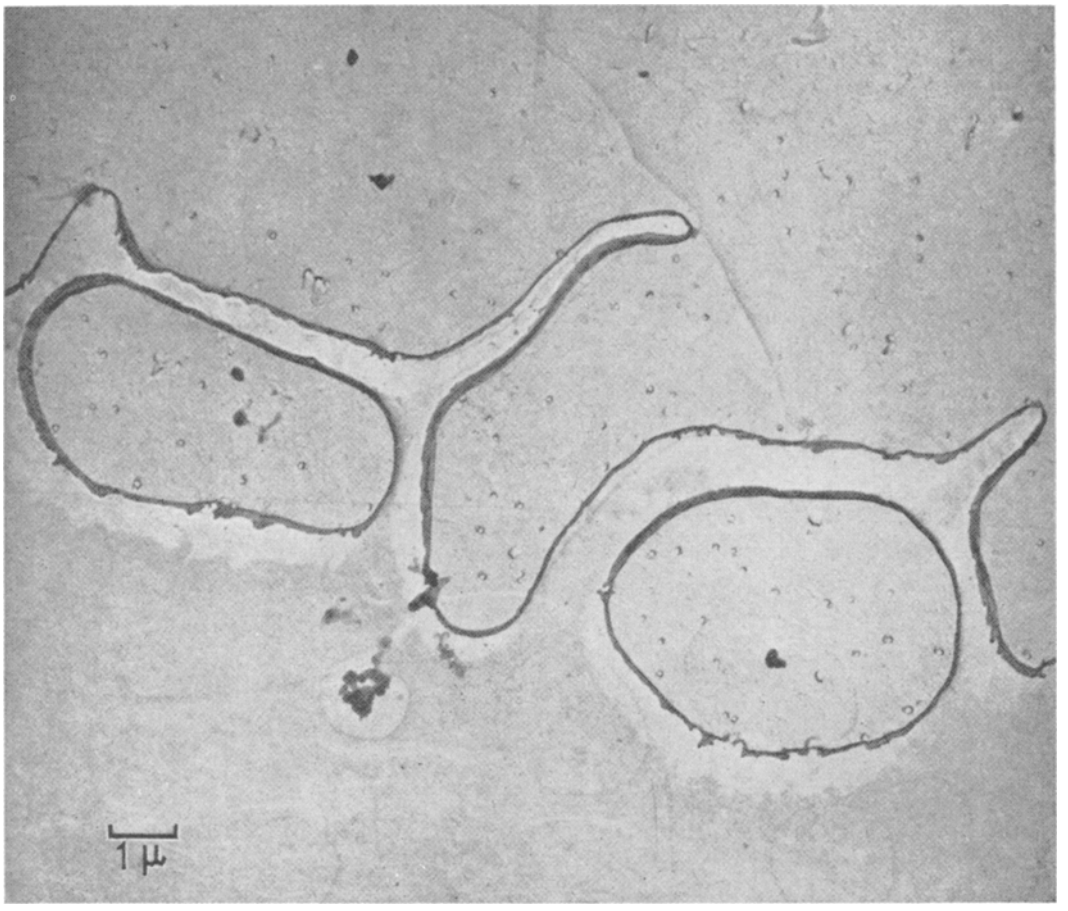

Figure 9 Quenched glass of composition 40% Nb_2O_5 : 60% $Na_2B_4O_7$.

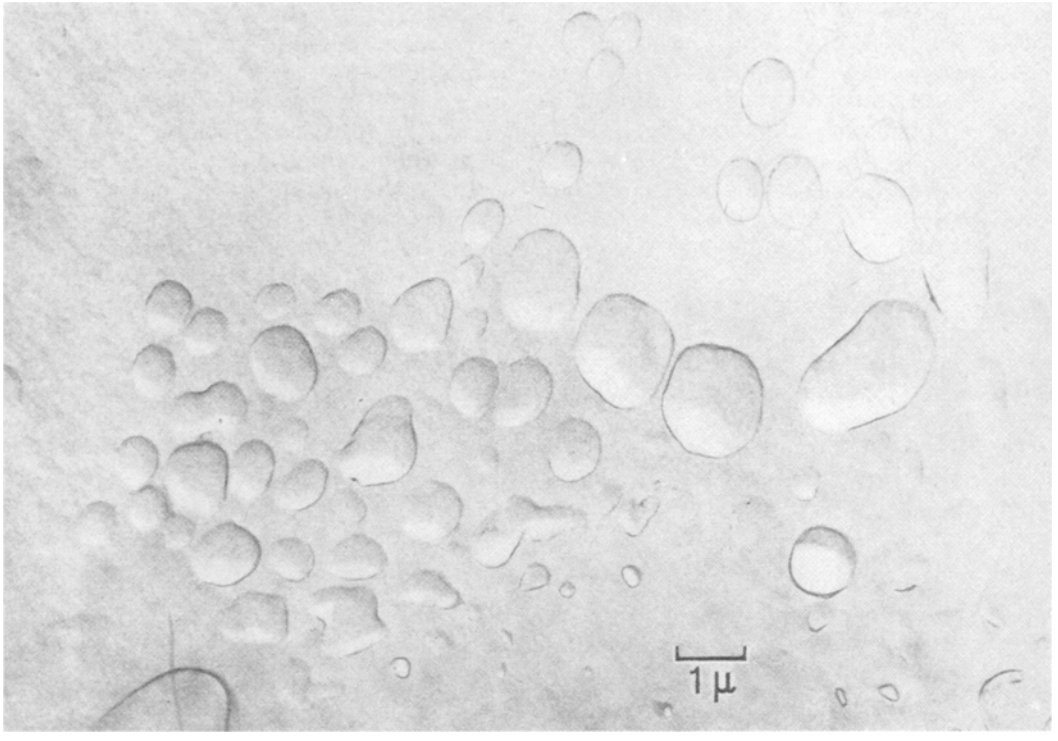

Figure 10 Quenched glass of composition 30% Nb_2O_5 : 70% $Na_2B_4O_7$.

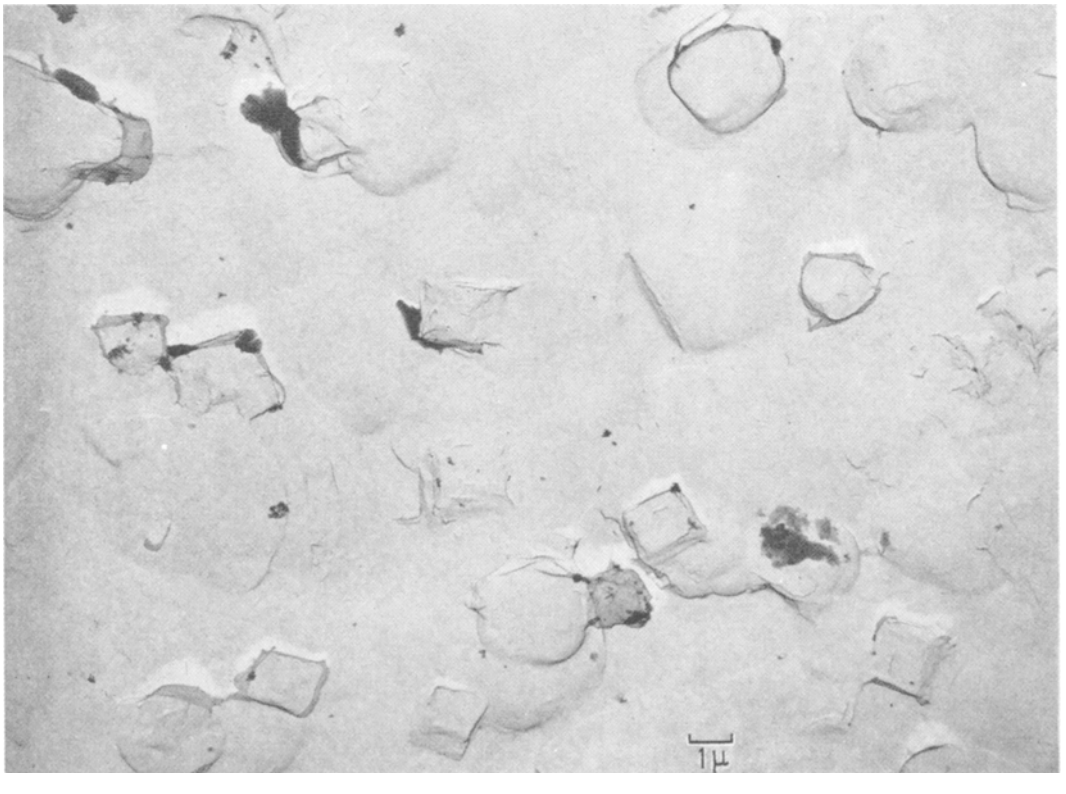

Figure 11 Initial stages of $NaNbO_3$ growth from 30% Nb_2O_5 : 70% $Na_2B_4O_7$.

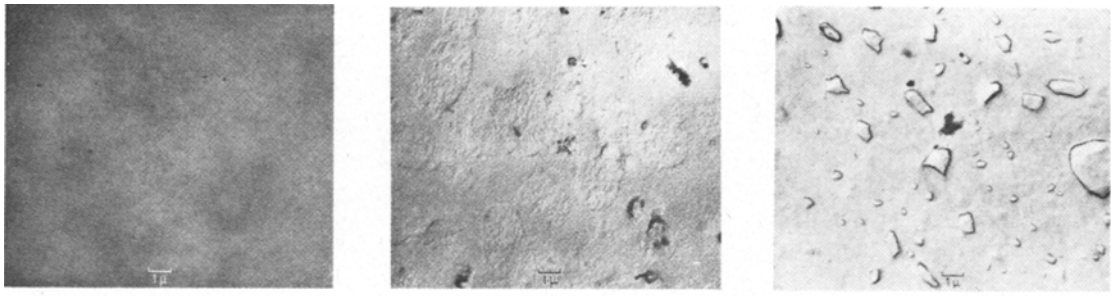

Figure 12 (a) Homogeneous borate-rich glass heat treated at 600° C. (b) Developing structure in borate-rich glass heat treated at 675° C. (c) $Na_2B_4O_7$ crystals growing from borate-rich glass.

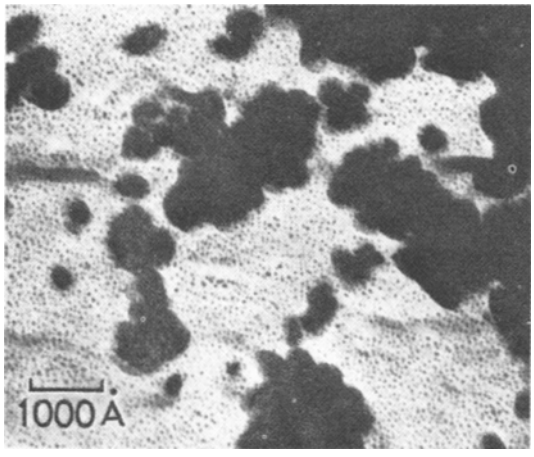

Figure 13 Electron micrograph of glass bead (40% Nb_2O_5: 60% $Na_2B_4O_7$) quenched in hot-stage microscope (μDTA) from 600° C.

cubic primary crystals of sodium niobate from the melt.

Nucleation and growth almost invariably occurred on the surface of the microdroplets, so reducing the inaccuracies in size measurements which must be present in some degree due to the curvature of the specimens. Thermal conditions were readily manipulated until several micro-crystals were observed to form and remain stable. The microfurnace was then adjusted to the temperature at which growth rate was to be recorded. Photographs were taken with a 35-mm auto camera, with a constant time interval between frames. A typical crop of growing crystals from a 20% Nb_2O_5 : 80% $Na_2B_4O_7$ melt is shown in fig. 14. Measurement of crystal edge lengths were made from scaled print enlargements (×80), the values being averaged for all the crystals in view.

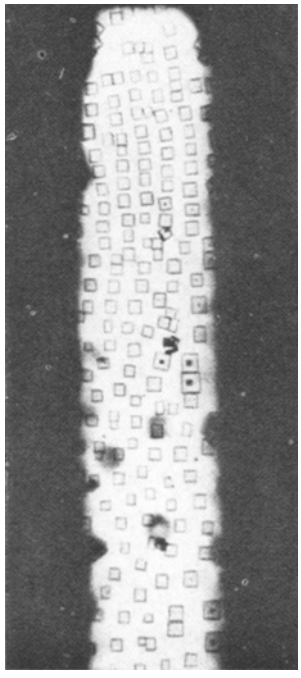

Figure 14 Crop of $NaNbO_3$ crystals growing from 20% Nb_2O_5 : 80% $Na_2B_4O_7$ melt.

Plots of average crystal width against time were linear for the early stages of growth (fig. 15), allowing a plot to be made of initial growth rate against temperature. This plot (fig. 16) is of a form typical of a logarithmic relation between growth rate, viscosity and degree of under-cooling. *Viz*, $\log R\eta/A = B \log \Delta T$, where: A and B are empirical constants; R is the growth rate; η the viscosity; ΔT the under-cooling from the liquidus temperature (see, for example, the discussion by Morley [10]).

The relatively high growth rates (2 to 5 μm/

sec) shown for the 20% Nb_2O_5 composition were typical over the area of the phase diagram where sodium niobate was the primary phase.

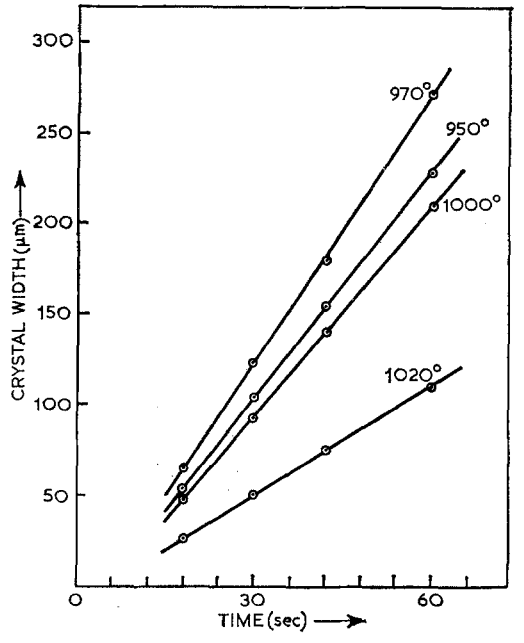

Figure 15 Linear temperature/time relationships on an average crystal width of cubic $NaNbO_3$ growing from 20% Nb_2O_5 : 80% $Na_2B_4O_7$ melt.

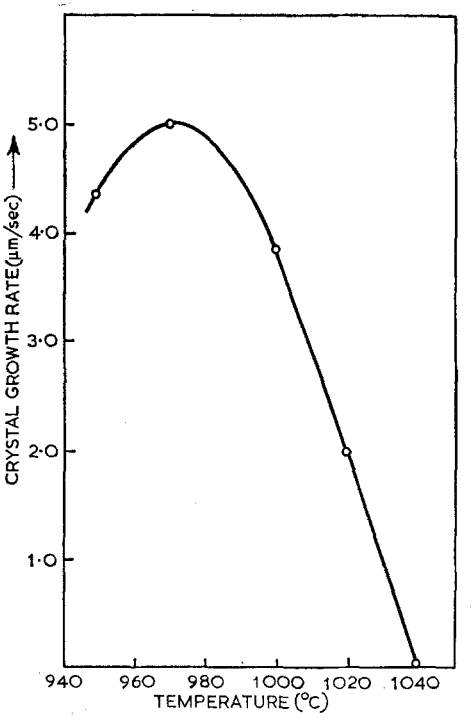

Figure 16 Crystal growth rate against temperature curve of $NaNbO_3$ (cubic) from 20% Nb_2O_5: 80% $Na_2B_4O_7$ melt.

4. Discussion

Although incomplete, the present study establishes that there is a potentially useful area in the $Na_2O/B_2O_3/Nb_2O_5$ ternary system bounded by the pseudo-binaries $NaBO_2/NaNbO_3$ and $Na_2O.4B_2O_3/NaNbO_3$ from which single crystals of sodium niobate may be grown. More requires to be done to increase understanding of nucleation and other precrystallisation phenomena in these melts and glasses, particularly in relation to unmixing processes which have recently assumed a more general practical significance in the field of glass-ceramic materials. Microphase separation has frequently been discussed in terms of competitive interaction of the cations with the anionic entities present. In this respect the ion-oxygen attraction, expressed as either field strength or ionic potential (cation charge/cation radius), has proved a useful, if qualitative, parameter for assessing the relative power of a cation to satisfy its co-ordination requirements and to dictate the configuration, ionic species and extent of immiscibility [11].

Such cation influence on structural behaviour

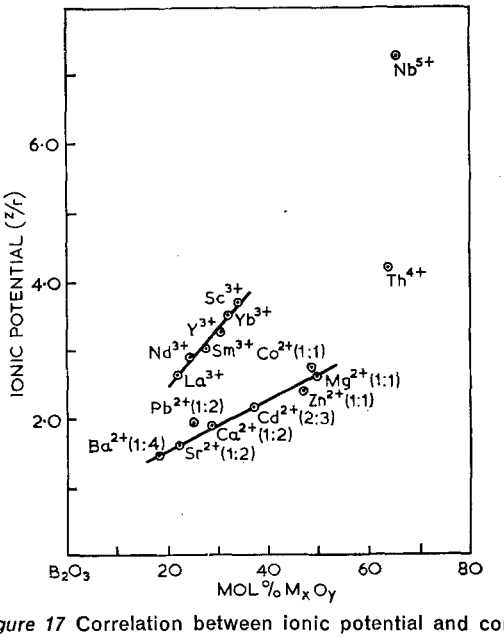

Figure 17 Correlation between ionic potential and concentration of metal oxide required to terminate liquid immiscibility.

in binary metal oxide/B_2O_3 systems can be illustrated by data from published phase

diagrams (see fig. 17). In the systems considered, very small additions of metal oxide bring about the onset of immiscibility, and the extent of the miscibility gap is found to be a function of ion oxygen attraction. Fig. 17 shows this concentration limit of metal oxides to increase with increasing field strength, i.e. the miscibility gap is widened. This is taken to reflect the increasing ability of cations of high field strength to successfully compete with B^{3+} for their oxygen co-ordination requirements. Free energy is then lowered by formation of a B_2O_3-rich network, and a cation-rich liquid, in which it would be expected that the size and complexity of the associated anion units would be cation dependent. That this is the case can be inferred from the structures that emerge as the primary phase under the two liquid regions of the divalent series in fig. 17. These structures are indicated in parenthesis on the figure as the ratio of metal oxide:B_2O_3. It is known that as the ratio of $MO:B_2O_3$ increases in crystalline borates, the size of the polyanionic network decreases [12].

In the case of Nb^{5+}, the primary phase under the two liquid region is Nb_2O_5, whereas for Th^{4+} it is $ThO_2.B_2O_3$. The general pattern is one of increasing degree of polymerisation in the anionic units as the field strength of the cation falls.

Before considering some inferences which may be drawn from the phase behaviour observed in the ternary system $Na_2O/B_2O_3/Nb_2O_5$, it must be emphasised that melts and glasses containing boric oxide as a component, present special problems when structural interpretations of their chemical and physical properties are attempted. There are fundamental uncertainties about the crystal/melt relationships involved when B_2O_3 itself melts, uncertainties which stem from the doubtful co-ordination state of the B^{3+} ion. The view generally held [13] is that much of the melt or glass structure comprises interlocking networks of triangularly co-ordinated boroxal groups with B-O-B bridging at each corner. It is the microstructure that results when this uncertainly constituted network is modified or fragmented by the addition of other metal oxides, that determines the properties and influences the phase behaviour of the resulting melts and glasses.

Reference to table I indicates that with regard to reactions in sodium diborate melts, niobium (and tantalum) present an anomaly in relation to other oxides of metals having inert gas type configuration. Passing from the oxides of more weakly interacting cations (La^{3+} and Y^{3+}) which form borates, the expected pattern whereby the cations of higher field strength strongly bond their near neighbour oxygen ions and re-precipitate as oxides, is not followed in the case of Nb^{5+} and Ta^{5+}. In speculating on the basic reasons for this difference, it seems significant that the structure of Nb_2O_5 (high temperature monoclinic form) is highly assymetric compared to ZrO_2 (fluorite structure at high temperature) and MoO_3 (octahedral layered). According to Gatehouse and Wadsley [14] the monoclinic Nb_2O_5 is constructed of two groups of differing sized NbO_6 octahedra with one niobium in every twenty-eight positioned in a tetrahedral site. The Nb-O distances through the structure vary between 1.73 and 2.26 Å. It is plausible to propose, therefore, that in the $Na_2B_4O_7/Nb_2O_5$ system, the overriding factor causing a decrease in free energy is the stabilisation of Nb^{5+} in the highly symmetrical perovskite structure. Suggestive support for this argument also arises from the observed phase relationships in the Nb_2O_5/B_2O_3 binary system. If it is assumed that in this system the niobium-ions are already striving for the perovskite configuration, then the first additions of B_2O_3 could provide the necessary oxygen-ions. Although B^{3+} has a higher field strength, the high concentration of Nb^{5+} ions would enable them to compete for the necessary co-ordination, charge balance being maintained by the B^{3+} ions. When the niobium-ions are satisfied, further addition of B_2O_3 results in the formation of an uncharged network and immiscibility arises, because of the incompatibility between this and the ionic "perovskite" phase. If this model is valid the expected O:Nb ratio in the niobium-rich phase should be close to 3:1. Following Levin [11] this ratio can be independently calculated from the phase diagram, knowing that the composition of the niobium-rich phase is 65.7 mole % Nb_2O_5: 34.3 % B_2O_3. It follows that the O:Nb ratio is

$$\frac{(5 \times 0.657) + (3 \times 0.343)}{(2 \times 0.657)} = 3.28$$

In spite of the presumptive nature of the reasoning, the agreement seems too close to be completely fortuitous.

References

1. L. E. CROSS and B. J. NICHOLSON, *Phil. Mag.* **46** (1955) 453.
2. R. H. DUNGON and R. D. GOLDING, *J. Amer. Ceram. Soc.* **47** (1964) 73.
3. J. H. WELCH, *J. Sci. Instr.* **31** (1954) 458.
4. R. P. MILLER and G. SOMMER, *ibid*, **43** (1966) 293.
5. R. K. BAYLISS and R. DERRY, *J. Appl. Chem.* **16** (1966) 114.
6. B. NADOR, *Nature* **201** (1964) 291.
7. G. W. MOREY and H. E. MERWIN, *J. Amer. Chem. Soc.* **58** (1936) 2258.
8. M. W. SHAFER and R. ROY, *J. Amer. Ceram. Soc.* **42** (1959) 485.
9. E. M. LEVIN, *J. Res. Nat. Bur. Stand.* **70A** (1966) 11.
10. J. G. MORLEY, *Glass Tech.* **6** (1965) 69, 77.
11. E. M. LEVIN, *J. Amer. Ceram. Soc.* **50** (1967) 29.
12. J. KROGH-MOE, *Phys. Chem. Glasses* **1** (1960) 26.
13. *Idem, ibid* **3** (1962) 1.
14. B. M. GATEHOUSE and A. D. WADSLEY, *Acta. Cryst.* **17** (1964) 1545.